AD

TECHNICAL REPORT ARLCB-TR-84004

AN EXPERIMENTAL STUDY OF PERFORATED MUZZLE BRAKES

ROBERT E. DILLON Jr.

HENRY T. NAGAMATSU

FEBRUARY 1984

US ARMY ARMAMENT RESEARCH AND DEVELOPMENT CENTER
LARGE CALIBER WEAPON SYSTEMS LABORATORY
BENET WEAPONS LABORATORY
WATERVLIET N.Y. 12189

APPROVED FOR PUBLIC RELEASE; DISTRIBUTION UNLIMITED

DISCLAIMER

The findings in this report are not to be construed as an official Department of the Army position unless so designated by other authorized documents.

The use of trade name(s) and/or manufacture(s) does not constitute an official indorsement or approval.

DISPOSITION

Destroy this report when it is no longer needed. Do not return it to the originator.

SECURITY CLASSIFICATION OF THIS PAGE (When Data Entered)

REPORT DOCUMENTATION PAGE	READ INSTRUCTIONS BEFORE COMPLETING FORM
1. REPORT NUMBER: ARLCB-TR-84004	2. GOVT ACCESSION NO.: AD-A139766
3. RECIPIENT'S CATALOG NUMBER	
4. TITLE (and Subtitle): AN EXPERIMENTAL STUDY OF PERFORATED MUZZLE BRAKES	5. TYPE OF REPORT & PERIOD COVERED: Final
	6. PERFORMING ORG. REPORT NUMBER
7. AUTHOR(s): CPT Robert E. Dillon, Jr. Henry T. Nagamatsu (RPI, Troy, NY)	8. CONTRACT OR GRANT NUMBER(s)
9. PERFORMING ORGANIZATION NAME AND ADDRESS: US Army Armament Research & Development Center Benet Weapons Laboratory, DRSMC-LCB-TL Watervliet, NY 12189	10. PROGRAM ELEMENT, PROJECT, TASK AREA & WORK UNIT NUMBERS: AMCMS No, 2080.15.6000.0 PRON No. 1A1221B81A1A
11. CONTROLLING OFFICE NAME AND ADDRESS: US Army Armament Research & Development Center Large Caliber Weapon Systems Laboratory Dover, NJ 07801	12. REPORT DATE: February 1984 13. NUMBER OF PAGES: 33
14. MONITORING AGENCY NAME & ADDRESS (if different from Controlling Office)	15. SECURITY CLASS. (of this report): Unclassified
	15a. DECLASSIFICATION/DOWNGRADING SCHEDULE

16. DISTRIBUTION STATEMENT (of this Report)

Approved for public release, distribution unlimited

17. DISTRIBUTION STATEMENT (of the abstract entered in Block 20, if different from Report)

18. SUPPLEMENTARY NOTES: To be presented at the 17th Fluid Dynamics, Plasma Dynamics & Laser Conference, Snowmass, CO, 25 - 27 June '984, sponsored by the AIAA.

19. KEY WORDS (Continue on reverse side if necessary and identify by block number)
Perforated Muzzle Brake
Muzzle Blast
Shock Wave

20. ABSTRACT (Continue on reverse side if necessary and identify by block number)

A firing test was conducted to examine the recoil efficiency and blast characteristics of perforated muzzle brakes fitted to a 20-mm cannon. Recoil impulse blast overpressures, muzzle velocity, sequential spark shadowgraphs, and photographs of the muzzle flash structure were obtained. Three different muzzle devices were used with one device equipped with pressure transducers to measure the static pressure in the brake. Experimental results are compared with the earlier predictions of Dillon and Nagamatsu.

DD FORM 1 JAN 73 1473 EDITION OF 1 NOV 65 IS OBSOLETE

UNCLASSIFIED

SECURITY CLASSIFICATION OF THIS PAGE (When Data Entered)

TABLE OF CONTENTS

TABLES

LIST OF ILLUSTRATIONS

ACKNOWLEDGEMENTS

The authors wish to thank Dr. Edward Schmidt and his associates at BRL's Fluid Physics Branch for their generous assistance in conducting the firing tests. The authors are especially grateful to Messrs. Ed Baur, Bill Thompson, Don McClellan, and John Carnahan.

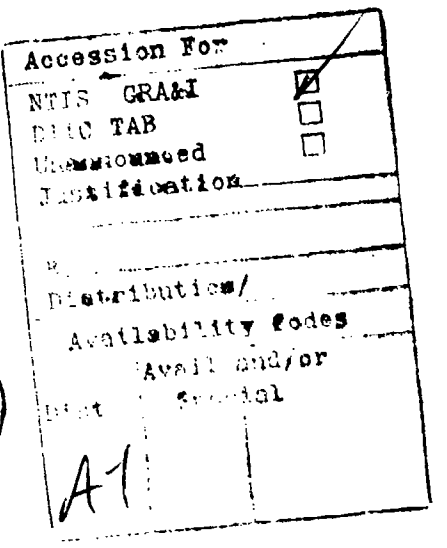

INTRODUCTION

Recent trends in the development of light armored assault vehicles (LAV) equipped with high velocity tank cannon have initiated a need for a medium efficiency muzzle brake. The principle function of the muzzle brake is to reduce the recoil impulse to a level that is acceptable for a light assault vehicle. Equally important is the need for accuracy and lightweight. Because of the accuracy criterion, the muzzle brake must not adversely alter the exterior ballistic trajectory and thereby affect weapon precision. The brake must be capable of accommodating both fin and spin stabilized kinetic energy rounds. Since the LAV has an overall system weight limit due to air transportability requirements, the muzzle brake likewise has a weight constraint. Based upon the considerations mentioned, the most promising approach appears to be a perforated muzzle brake.

Reference 1 presents a numerical procedure for predicting the performance of perforated muzzle brakes. The present report describes a firing test conducted to study the performance of these devices. The experimental results reported here will be a useful aid in refining the numerical procedure set forth in Reference 1 and in studying the performance of these devices.

There are numerous reports which describe experimental efforts at analyzing the performance of many different types of muzzle devices (refs 2-21), but no quantitative details have been reported on the functioning of perforated devices.

References are listed at the end of this report.

DESCRIPTION OF THE EXPERIMENT

A program was conducted to obtain experimental data on perforated muzzle brakes. These data would be used in a comparison of the predictions of brake performance described in Reference 1. Tests were conducted in the Aerodynamics Range of the Army's Ballistic Research Laboratory at Aberdeen Proving Ground, Maryland (ref 22). The firing tests were conducted to measure the free field blast overpressures around the weapon and the recoil impulse of the weapon fitted with different muzzle brakes. The blast and near muzzle flow field were further analyzed by taking spark shadowgraphs of the muzzle flow field at various times.

The free field blast around the muzzle was measured using an array of static pressure transducers placed on an arc .6 m (30 calibers) from the muzzle of the gun. The transducers were arranged on angles measured from the axis of the gun from 10 to 150 degrees. The transducers used were Kistler 20185 Piezotrons, or the equivalent, mounted in sharp edged semi-circular plastic discs having a diameter of .07 m. The discs were aligned such that the plane of their surface passed through the axis of the gun. The output of the transducers was recorded on magnetic tape after being processed by a Physical Data, Inc. Model 515A Transient Recorder and a Hewlett Packard 9845B Computer.

In addition to the free field blast pressure measurement, the recoil impulse was obtained utilizing a free recoil mount. This mount presents very little resistance to the rearward movement of the gun for a distance of about 0.1 m. By measuring the recoil velocity and knowing the mass of the recoiling parts, the total impulse can be determined. The recoil velocity was obtained

by displaying the interruptions of a helium neon laser beam directed through a calibrated grating fixed to the moving parts into a photodiode. The output of the photodiode was displayed on a Nicolet Model 204 digital oscilloscope. By measuring the time elasped between known distances of the grating, the recoil velocity was obtained. The recoil momentum was computed from this velocity.

Spark shadowgraphs were obtained by directing a one-microsecond spark light source onto a large Fresnel lens. The shadow caused by the flow field properties cast upon the Frensel lens was directed into the camera. A delay counter was used to trigger the spark light source at a specific time. This allowed the flow field to be observed at different times. This technique proved to be very useful in obtaining sequenced shadowgraphs of the flow field development (ref 4). An open shutter camera loaded with color film was used to monitor the flash characteristics and any secondary combustion in the exhaust flow.

The projectile velocity was measured at six stations from 4.6 m to 13.85 m measured from the muzzle of the gun. At each of these stations, a light screen was connected to a time interval counter. The projectile triggered the light screen which caused the time interval counter to stop. The velocity was obtained by recording the elapsed time between any two stations.

The weapon used in the firing tests is a 20 mm cannon with a shot travel of 1.43 m, a chamber volume of $4.17 \times 10^{-5} m^3$, and a twist of rifling of one turn in 25 calibers. The projectile is that of the standard M55A2 training round (inert) weighing 0.098 kg. The propellant for this round is WC870 ball powder with the following properties:

Specific Force = 9.8×10^5 m^2/s^2

$\gamma = 1.24$

The M55A2 round has .0389 kg of propellant which produces a nominal muzzle velocity of 1045 m/s with this gun. The test set-up is shown in Figure 1.

The results of three muzzle brake configurations will be reported. One brake was constructed to house three PCB model H113A23 pressure transducers to record inbore pressures. The output of these pressure transducers was recorded on a Nicolet Model 204 digital oscilloscope. These gages gave a record of the static pressure inside the brake during firing. The vent holes of this brake were aligned so that the interference from the exhausting gases on the transducer leads would be minimized. All brakes had vent holes of the following description: three rows of 1.6 mm diameter holes with twelve holes per row, three rows of 3.2 mm diameter holes with twelve holes per row, and four rows of 4.8 mm diameter holes with twelve holes per row. The vent holes were of constant diameter and were located perpendicular to the axis of the gun bore. The configuration produced a very simple brake with which to conduct the test. The brakes tested are described in Table I.

TABLE I. 20 mm MUZZLE DEVICES

Number	Description
1	Perforated Muzzle Brake, 21 mm Projectile Hole AR = 3.38 L/D = 5.75
2	Perforated Muzzle Brake, 21 mm Projectile Hole AR = 3.38 L/D = 10.7, 3 Static Pressure Taps
3	Perforated Muzzle Brake, 21 mm Projectile Hole AR = 3.38 L/D = 1.78

In Table I AR refers to the vent area ratio or

$$AR = \frac{AV}{AB}$$

where AV = Total vent area

AB = Bore area

and $L/D = \frac{\text{vent length}}{\text{vent diameter}}$

These two parameters are of importance in determining the recoil efficiency of these devices.

Conduct of the Experiment

The firing test began with a series of five shots with the bare muzzle configuration to establish the baseline data. Shots were then fired with each muzzle brake to obtain the data needed for comparison. This procedure provided good data to be used in the analysis of this design approach.

The test procedures followed were identical for every round fired. This standard procedure minimized error and observed rigid safety standards. For each shot the room was darkened, the shadowgraph and flash observation cameras were loaded, and the shutters opened. The gun was loaded and then moved to the most forward position in the recoil mount. In order to insure the gun was not fired with technicians in the firing room, each technician carried a key that had to be inserted into the firing console before the weapon would fire. When the firing room was loaded and cleared of personnel, the computer and oscilloscopes were armed for data acquisition. The velocity screens and the time interval counters were cleared and the firing sequence was initiated. Once initiated, the sequence started the time interval counters, set the spark

light source power supply, and fired the gun.

After each shot, a technician applied the necessary time delay setting for the spark light source and reloaded the cameras and gun. While the gun and cameras were reloaded, the oscilloscopes displayed their data and then stored it on a magnetic disk. The computer automatically displayed the blast pressure traces and produced hard copies. When the computer completed the last plot, it was armed for the next shot and the cycle was repeated. The flash monitoring photographs were polaroid and thus were quickly available. The spark shadowgraphs needed seven minutes for developing the film. This gave the crew enough time to repeat a shot in the event a shadowgraph was not obtained due to light failure or other reasons. This system worked very well and enabled many data to be acquired in a very short time.

Experimental Results

Free Field Blast

The free field blast was measured to determine the effects caused by the addition of the perforated muzzle brake. The blast pressures for each muzzle configuration are shown in Figures 2 through 4. The flow field generated by the various brakes was recorded via the spark shadowgraph technique.

The blast and flow fields generated by a perforated brake tested are shown in the following sequence of spark shadowgraphs. Figures 5 and 6 show the flow field 110 μs prior to shot ejection. In these figures, the precursor shock wave and plume details are readily visible. The flow field at 14 μs prior to shot ejection is shown in Figures 7 and 8. Note the propellant gas flow issuing from the first few rows of vent holes (see Figure 8). In Figures

9 and 10 the flow field is 139 μs from shot ejection, the projectile has cleared the muzzle, and the main propellant driven blast is forming. The fully developed blast flow is seen in Figures 11 and 12. These show the projectile out of the shock waves, the fully developed muzzle exhaust plume, and the high density gas cloud formed by the propellant gas as it discharges into the atmosphere from the vent holes.

Muzzle Brake Interior Pressure

The pressure in the interior of the muzzle brake was measured during the test. The output of the PCB pressure transducer for one shot is presented in the next set of figures. The output from gage #1 located at the entrance to the brake -.119 m from the muzzle of the brake, is shown in Figure 13. The weak pressure rise associated with the precursor is seen at early times followed by the sharp rise caused by the passage of the projectile. Once the projectile has passed the gage, the pressure decays due to the loss of mass through the muzzle brake.

The pressure history for the gage located -.064 m from the muzzle of the brake is shown in Figure 14. The pressure history follows the trend of the previous gage with the effects of the precursor, projectile passage, and blowdown. The peak pressure is seen to be lower from this second gage than for the first gage. This is due to the propellant gases being vented through the first six rows of vent holes located between these two gages.

The pressure history shown in Figure 15 is that of the third gage, located -.01 m from the exit of the muzzle brake. As seen in the previous muzzle brake pressure traces, this trace displays the features seen in the other two, i.e., precursor passage, and blowdown. The maximum pressure for

the third gage has dropped considerably from the level seen in the first gage. This indicates that a considerable amount of propellant gases have been vented through the holes in the brake.

Recoil Reduction

The recoil impulse was determined for every muzzle configuration used in the firing test. This was accomplished by utilizing the free recoil mount. The mount permits, as much as possible, free recoil of the weapon during firing. By measuring the output of the photodiode caused by the calibrated grating breaking a laser beam, the recoil velocity can be readily determined. Knowing the mass of the recoiling parts permits the momentum of the recoiling mass to be calculated. This momentum is equal in magnitude to the impulse generated from firing the gun.

The efficiency of the muzzle brake can be determined by measuring the recoil impulse for the brake and no brake configurations. The experimentally determined gas dynamic efficiency can be computed by

$$\beta = (I_{wo}-I_w)/(I_{wo}-M_pV_e)$$

where

I_{wo} = impulse without muzzle device

I_w = impulse with muzzle device

M_p = mass of projectile

V_e = projectile muzzle velocity

The term M_pV_e is the impulse associated with firing the projectile. When this is subtracted from I_{wo} the remainder is the residual impulse of the propellant gases available to do work on the brake. The overall recoil efficiency of the muzzle brake is given by

$$\psi = (I_{wo}-I_w)/I_{wo}$$

The experimental results for the brake efficiencies are presented in Table II. A further point of interest in Table II is the increase in muzzle velocity associated with the use of these muzzle brakes.

TABLE II. RECOIL AND VELOCITY DATA

Configuration	I_{wo} (N-s)	I_w (N-s)	ψ (%)	β (%)	V_{muz} (m/s)	Flash
20 mm Bare Muzzle	148	-	-	-	1044	No
#1	-	130	13	42	1058	No
#2	-	129	13	42	1060	No
#3	-	125	15	52	1058	No

DISCUSSION OF RESULTS

The blast overpressures for each muzzle configuration are shown in Figures 2 through 4. In these figures the shifting of the blast levels at each gage location is evident. Note that the blast overpressure with the perforated muzzle brake is higher along the axis of the gun than the bare muzzle case. At locations between 90° and 35° however, the blast overpressures are lower with the perforated muzzle brake. The increase in blast overpressure to the rear of the weapon is due to the radial venting of the propellant gases as opposed to the normally axial efflux encountered with the bare muzzle case. The increase in blast overpressures forward of 90° from the muzzle is due to the mechanism generating the blast wave, namely the opening of the brake vent holes. The projectile uncorks each row of vent

holes causing the propellant gases to vent and create a shock wave and plume structure. As the projectile passes each subsequent row of vents, a starting shock wave is created and the strength of the outer blast is increased. The focusing of the outer blast in the predominantly forward direction is the result of the sequential venting of the brake which tends to produce stronger blast in the forward direction.

The reduction of the blast overpressure in the lateral position of the muzzle, 35° - 90°, was not expected but follows from the previous observations. The amount of energy a weapon and cartridge combination can deposit to the atmosphere is fairly constant. If one raises blast overpressures in one area, it follows that the overpressure should be reduced in some other area. A further contribution to the lower blast overpressures in the lateral positions is presumed to be due to the geometry of the muzzle brake. The presence of the many holes presents a more diffuse energy source than a baffled brake configuration or the bare muzzle. This configuration then produces a weaker blast wave in the lateral positions. This phenomena was observed in Reference 33 with the supersonic jet noise. In Reference 1 the Godunov code predicted pressure increases over the bare muzzle case on the order of 70 percent at the 150° location due to the use of a perforated muzzle brake, cf. Figure 16. The measured pressure increase at this location was found to be 63 percent. This agreement is considered quite good considering the Godunov Code does not model the precursor effects, the boundary layer buildup and other viscous effects in the vent holes, and the turbulent mixing that occurs in the external jet flow field. All of these physical phenomena tend to attenuate the strength of the blast wave which puts the Godunov

predicted pressure in a much better perspective. For the purpose of this investigation and considering the assumptions made in applying the Godunov Code to this regime, this agreement is considered quite good.

The measured static pressures at each gage location in brake #2 are shown in Figures 13 through 15. These pressures follow the trend predicted by the Method of Characteristics (MOC) presented in Reference 1. The pressure at the first gage location, placed at the entrance to the brake, was measured to within 10 percent of the value calculated by the MOC. At the exit of the brake the agreement is not as good. The MOC underpredicted the pressure at the exit of the brake by about 49 percent. This discrepancy is seen to be attributed to the assumption made in applying the MOC to the flow in the muzzle brake. The MOC assumes a perfect gas and one-dimensional flow. The vent nozzles are assumed to open immediately upon projectile passage and flow fills the vent holes. The viscous and inertial effects such as boundary layer choking of the vents or the occurrence of separated flow near the upstream side of the vent-bore juncture are not modeled. The one-dimensional approximation does not take into account the cross bore gradients in the fluid properties caused by the venting outflow. All these assumptions lead to a higher mass outflow through the vent holes being predicted than that which is observed in the actual flow. This causes the MOC predictions of pressure to be lower at the exit of the brake than those seen experimentally.

An interesting trend was seen in the increase in the muzzle velocity with the addition of the muzzle brake. Table II presents the muzzle velocity for each configuration tested. The MOC predicted an increase in muzzle velocity of 2 m/s over the bare muzzle case for the brake tested in this firing test.

The actual brake produced muzzle velocities 13-15 m/s higher than the bare muzzle case. The causes of the MOC prediction to be lower were determined by those discussed in the previous paragraph. Since the MOC overpredicts the amount of propellant gases venting through the brake, it will underpredict the resultant muzzle velocity due to there being less propellant gase available to push the projectile. Nevertheless, the increase in muzzle velocity achieved by these brakes is seen to be of significance and is a favorable occurrence.

The recoil characteristics of each configuration are also presented in Table II. The MOC predictions of recoil impulse were typically lower than the experimentally determined values by about 13-17 percent. This level of agreement was achieved in all the measurable quantities concerning recoil impulse. The MOC predicted values for the muzzle brake efficiency were seen to be slightly higher than those determined experimentally. This was to be expected following the observed trends seen in the measured pressure inside the muzzle brake. The MOC predictions of the overall efficiency, ψ, were seen to be within 15 percent of the experimentally determined values. This agreement is considered quite good.

The MOC predicted values for the gas dynamic efficiency, β, was about 30 percent over that determined by experiment. This is an interesting departure from the usual 13-17 percent trend in the other error observed. The most probable explanation for this lies in the computation of β. β is determined by

$$\beta = \frac{\overset{(-13)}{(I_{wo}} - \overset{(-14)}{I_w)}}{\underset{(-13)}{(I_{wo}} - \underset{(-4)}{M_p V_o)}}$$

ψ is determined by

$$\psi = \frac{\overset{(-13)}{I_{wo}} - \overset{(-14)}{I_w}}{\underset{(-13)}{I_{wo}}}$$

The error associated with each constituent quantity is shown in parenthesis. It is clear that the computation of β has an unbalanced error which is seen to be additive over the existing error between prediction and experiment. The computation for ψ has error, but since it is associated with all the quantities in ψ is of the same value, the error cancels out and closer agreement is obtained.

An interesting observation is the reduction of brake efficiency that occurs with larger wall thicknesses, as shown in Table II. Brake #1 has L/D = 5.75 as opposed to brake #3 with L/D = 1.78. The efficiency reduction due to the thickness of the walls is presumed to be due to either the added wall friction or the buildup of pressure on the upstream wall of the vent hole. In either case, this occurrence will be looked at more closely.

The agreement of all the numerical predictions with the experimental values is quite good. The models used in the analysis are seen to adequately describe most of the flow regimes.

CONCLUSIONS

The experimentally measured quantities of the performance of the perforated muzzle brakes was found to validate the numerical predictions presented in Reference 1. The simplifying assumptions made in order to apply the MOC to this flow regime were found to cause higher predictions in muzzle

brake efficiency than those found by experiment. The experimental results give good indications as to how to modify the current model to better predict the performance of the devices.

The experiments further verified the capabilities of the Godunov scheme developed in Reference 24. The experimental results have revealed an accurate modeling of the flow field by the Godunov Code in Reference 1. As was found with the MOC results, the assumptions made in applying the Godunov Code caused the predicted results to vary from the experimental results in an anticipated direction. The Godunov Code is a valuable tool in predetermining the blast field structure and signature for these type of muzzle brakes.

The simple perforated muzzle brakes were found to be a useful muzzle device both in terms of producing a satisfactory braking force and in modifying the blast signature of the weapon exhaust field. The perforated brakes tested, as anticipated, did not produce any flash.

The perforated brakes studied produced an increase in projectile velocity by 13-15 m/s. This amounts to a 1.5 percent increase in the muzzle velocity which is a desirable effect.

The perforated muzzle brakes tested were observed to produce a weaker muzzle exhaust plume because of the propellant venting out of the brake. This is seen as a favorable occurrence, as the reduced plume strength is presumed to have a favorable effect on the initial yaw rates of the projectile and on the projectile stability in the intermediate ballistic region (ref 25).

The perforated brakes used in this study did not experience any observable wear or erosion due to the hot (1705°K) propellant gases. This is

a favorable observation since reduced wear of these devices can result in the use of lighter materials and/or an increased service life.

The strong dependence of muzzle brake efficiency on the wall thickness or L/D ratio was significant enough to require an examination of it to determine the optimal wall thickness for a given brake design.

REFERENCES

1. Dillon, R. E. and Nagamatsu, H. T., "A Method of Analyzing Perforated Muzzle Brake Performance," ARDC Technical Report No. ARLCB-TR-84002, Benet Weapons Laboratory, Watervliet, NY, February 1984.

2. Oswatitsch, K., "Flow Research to Improve the Efficiency of Muzzle Brakes," (a) "Part I: Tests on Baffle Surfaces With One-Dimensional Flow," German Air Research Report 6601, 1943; (b) "Part II: Efficiency Factor, Momentum Relation, Two-Dimensional Flow, and Flow With Covering," Army Ordnance Report 1001, 1944; (c) "Part III: The Axial Symmetric Flow Problem, A Comparison of Tests of Muzzle Brakes Free of Reaction," Gottingen, 1945.

3. Schmidt, E. and Shear, D., "Flow Field About the Muzzle of an M16 Rifle," U.S. Army Ballistic Research Laboratory Report 1692, Aberdeen, MD, 1974.

4. Schmidt, E. and Shear, D., "Optical Measurements of Muzzle Blast," AIAA Journal, 13, 1086-1091 (1975).

5. Schmidt, E., Gion, E. J., and Shear, D., "Acoustic Thermometric Measurements of Propellant Gas Temperatures in Guns," AIAA Journal, 15, 222-226 (1977).

6. Gion, E. J. and Schmidt, E., "Measurement on a Circular Plate Immersed in Muzzle Flow," U.S. Army Ballistic Research Laboratory Report MR-2762, Aberdeen, MD, 1977.

7. Schmidt, E. and Gion, E. J., "Muzzle Blast of a 30 mm Cannon," U.S. Army Ballistic Research Laboratory Report ARBRL-MR-62805, Aberdeen, MD, 1978.

8. Schmidt, E. Gion, E. J., and Fansler, K. S., "A Parametric Study of the Muzzle Blast From a 20 mm Cannon," U.S. Army Ballistic Research Laboratory Report ARBRL-TR-02355, Aberdeen, MD, 1981.

9. Schmidt, E., "Secondary Combustion in Gun Exhaust Flows," U.S. Army Ballistic Research Laboratory Report ARBRL-TR-02373, Aberdeen, MD, 1981.

10. Schmidt, E. and Thompson, W. D., "The Effect of Muzzle Device Configuration on the Blast Overpressure Levels on the AH-1S Helicopter Tow Sight Unit," U.S. Army Ballistic Research Laboratory Report 747, Aberdeen, MD, 1982.

11. Soo Hoo, G. and Yagla, J., "Use of a Conical Muzzle Device to Control Gun Blast," Naval Weapons Laboratory Report TR-2793, Dahlgren, VA, 1972.

12. Soo Hoo, G., "Gun Blast Experiments With an 8"/51 Gun," Naval Surface Weapons Center Note NSWC/DL T-175, Dahlgren, VA, 1975.

13. Goss, C., "Reduced Scale Muzzle Brake Development for Marine Corps 203 mm Lightweight Howitzer," Naval Surface Weapons Center Report NSWC/DL TR-3420, Dahlgren, VA, 1976.

14. Pater, L. and Shea, J., "Use of Foam to Reduce Gun Blast Noise Levels," Naval Surface Weapons Center Report NSWC TR-81-94, Dahlgren, VA, 1981.

15. Pater, L. and Shea, J., "Techniques for Reducing Gun Blast Noise Levels: An Experimental Study," Naval Surface Weapons Center Report NSWC TR-81-120, Dahlgren, VA, 1981.

16. Pater, L., "Use of Aqueous Foam to Reduce Shoulder Launched Rocket Noise Level: Feasibility Investigation," Naval Surface Weapons Center Report NSWC TR-81-268, Dahlgren, VA, 1981.

17. G. Miller, et al., "Reduction of 5"/54 Gun Blast Overpressure by Means of an Aqueous Foam-Filled Muzzle Device," Naval Surface Weapons Center Report NSWC TR-81-128, Dahlgren, VA, 1981.

18. Smith, F., "Model Experiments on Muzzle Brakes," Royal Armament Research and Development Establishment Report 2/66, Ft. Halstead, UK, 1966.

19. Smith, F., "Model Experiments on Muzzle Brakes, Part III: Measurement of Pressure Distribution," Royal Armament Research and Development Establishment Report 3/68, Ft. Halstead, UK, 1968.

20. Pater, L., "Scaling of Muzzle Brake Performance and Blast Field," Naval Weapons Laboratory Report AD/A-001275, Dahlgren, VA, 1975.

21. Pater, L., "Muzzle Brake Parameter Study," Naval Surface Weapons Center Report TR-3255, Dahlgren, VA, 1975.

22. Braun, W., "The Free Flight Aerodynamics Range," U.S. Army Ballistic Research Laboratory Report 1048, Aberdeen, MD, 1958.

23. Nagamatsu, H. T. and Sheer, R. E. Jr., "Subsonic and Supersonic Jets and Supersonic Suppressor Characteristics," Aeroacoustics: Jet and Combustion Noise; Duct Acoustics (H. T. Nagamatsu, Ed.), Vol. 37 of Progress in Aeronautics and Astronautics (M. Summerfeld, Series Editor), AIAA, New York, 1975.

24. Widhoff, G., Buell, J., and Schmidt, E., "Time Dependent Near Field Muzzle Brake Flow Simulations," AIAA Paper 82-0973, presented at AIAA/ASME Third Joint Thermophysics, Fluids, Plasma, and Heat Transfer Conference, St. Louis, MO, June 1982.

25. Schmidt, E., "Measurement of Sabot Discard and Analysis of Associated Launch Disturbances," U.S. Army Ballistic Research Laboratory Report ARBRL-TR-02157, Aberdeen, MD, April 1979.

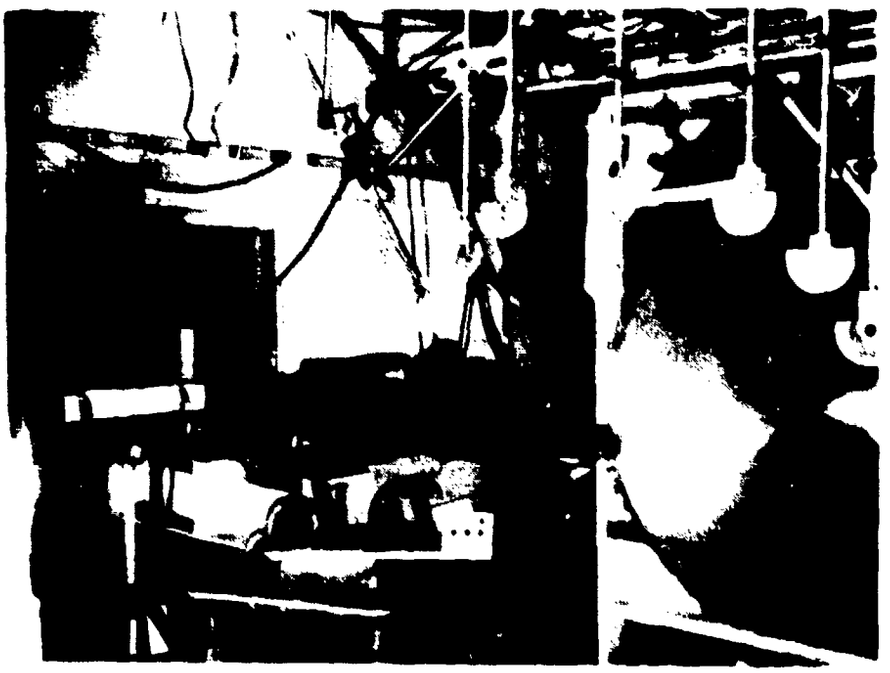

Figure 1. 20 mm Experimental Setup.

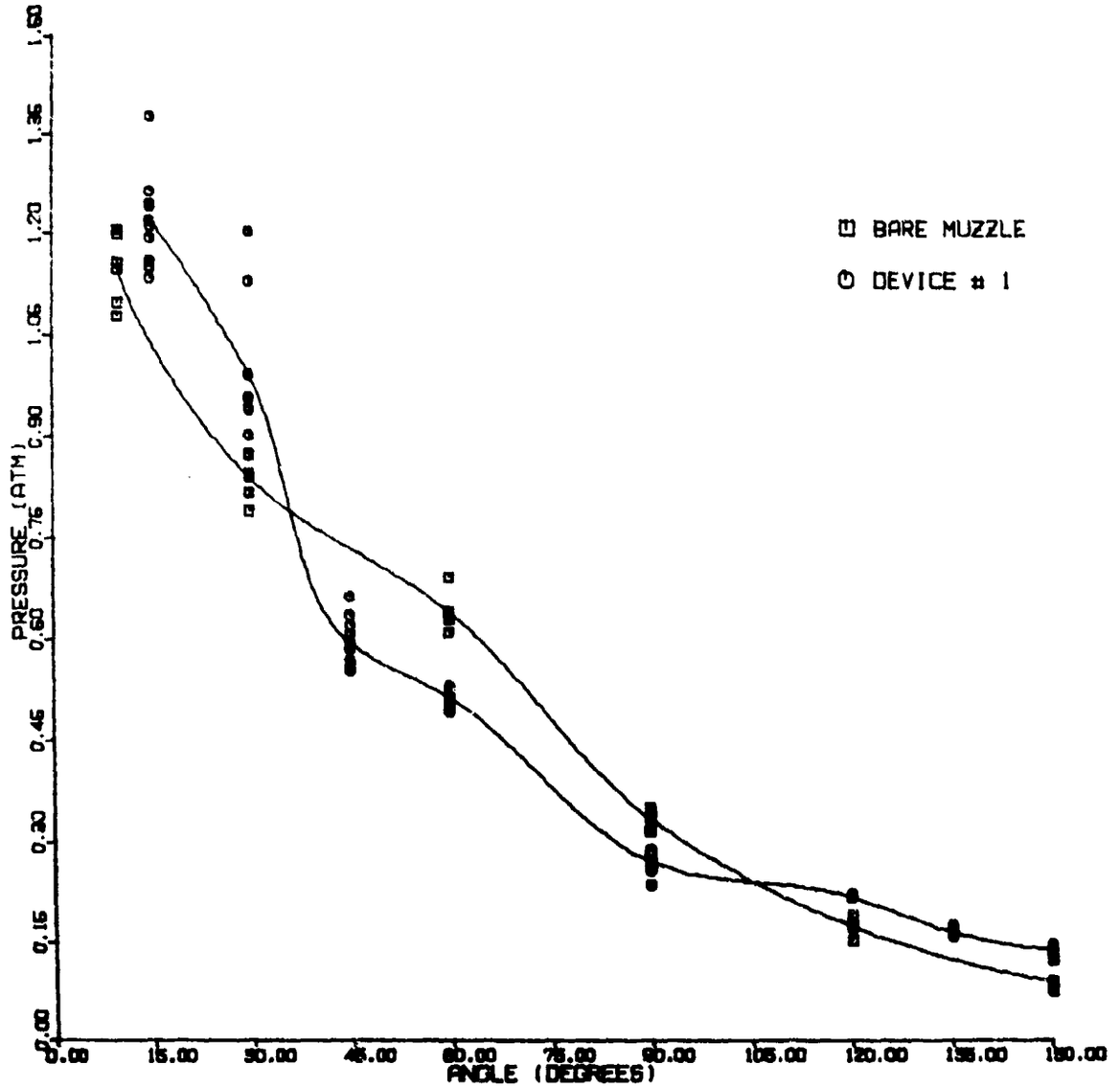

Figure 2. Blast Overpressure Measurements for Device #1.

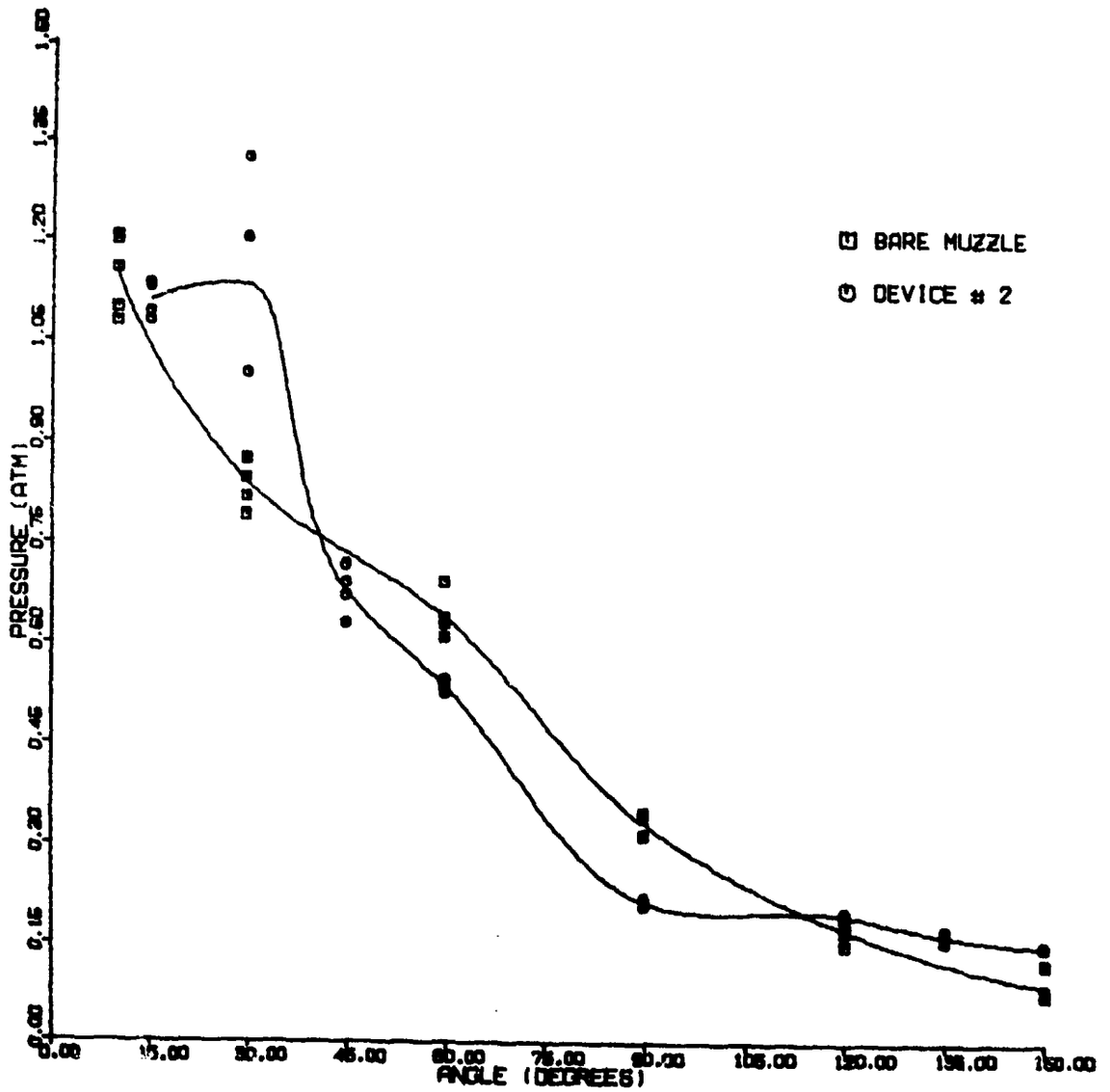

Figure 3. Blast Overpressure Measurements for Device #2.

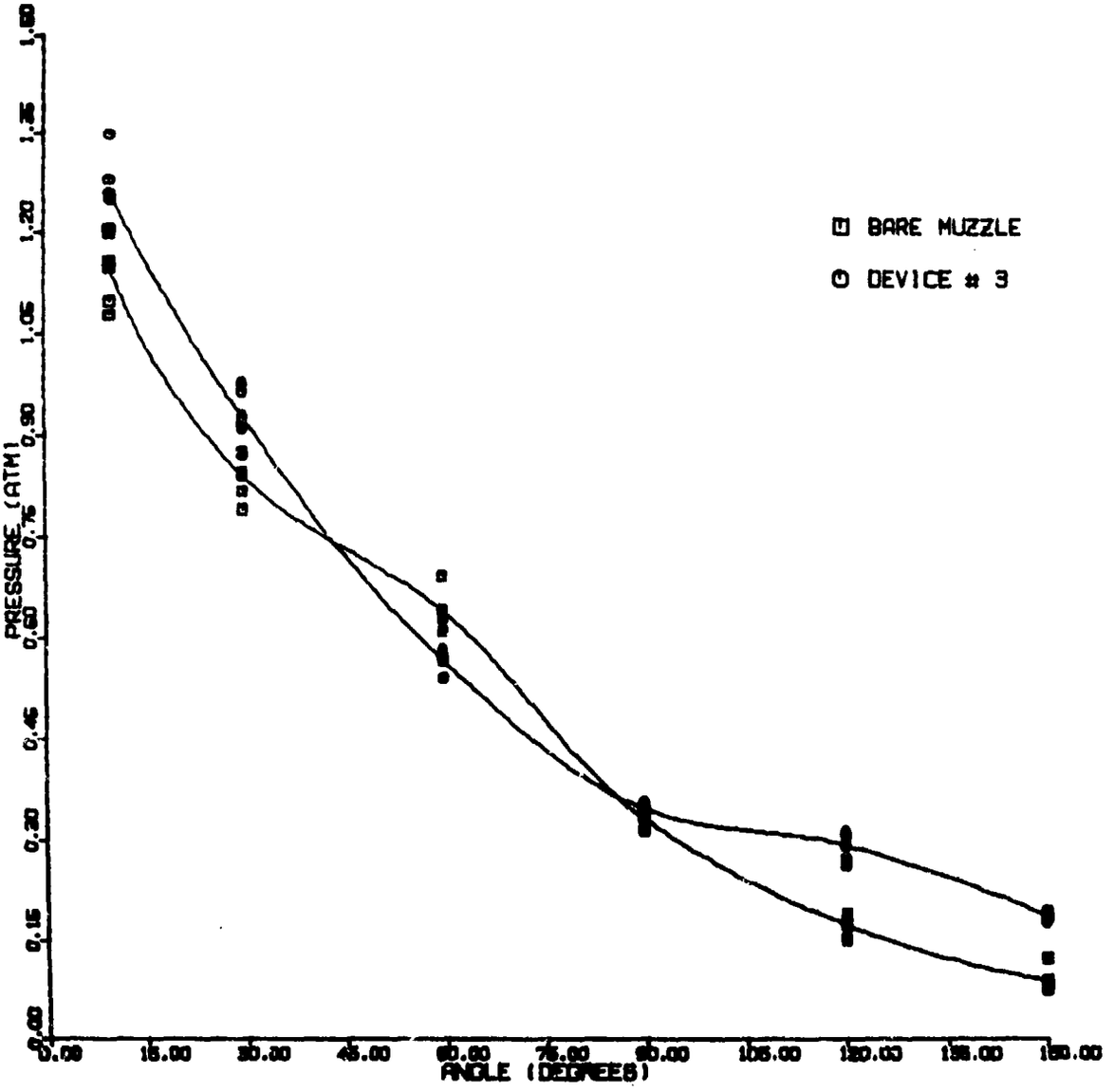

Figure 4. Blast Overpressure Measurements for Device #3.

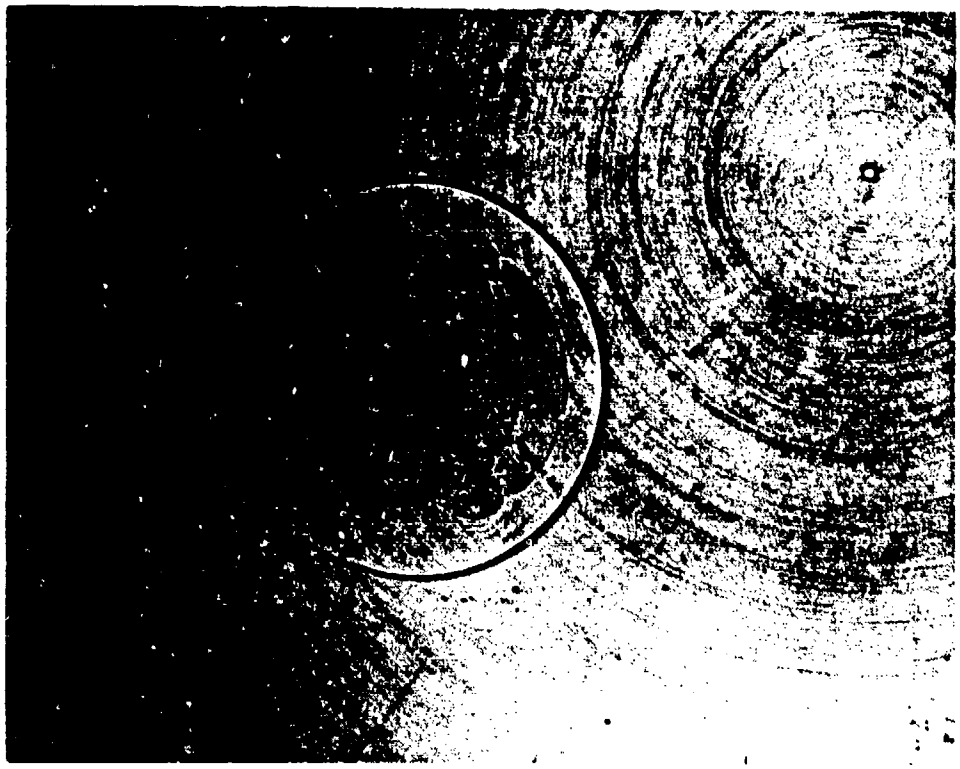

Figure 5. Spark Shadowgraph of Flow Field -110 μs Bare Muzzle.

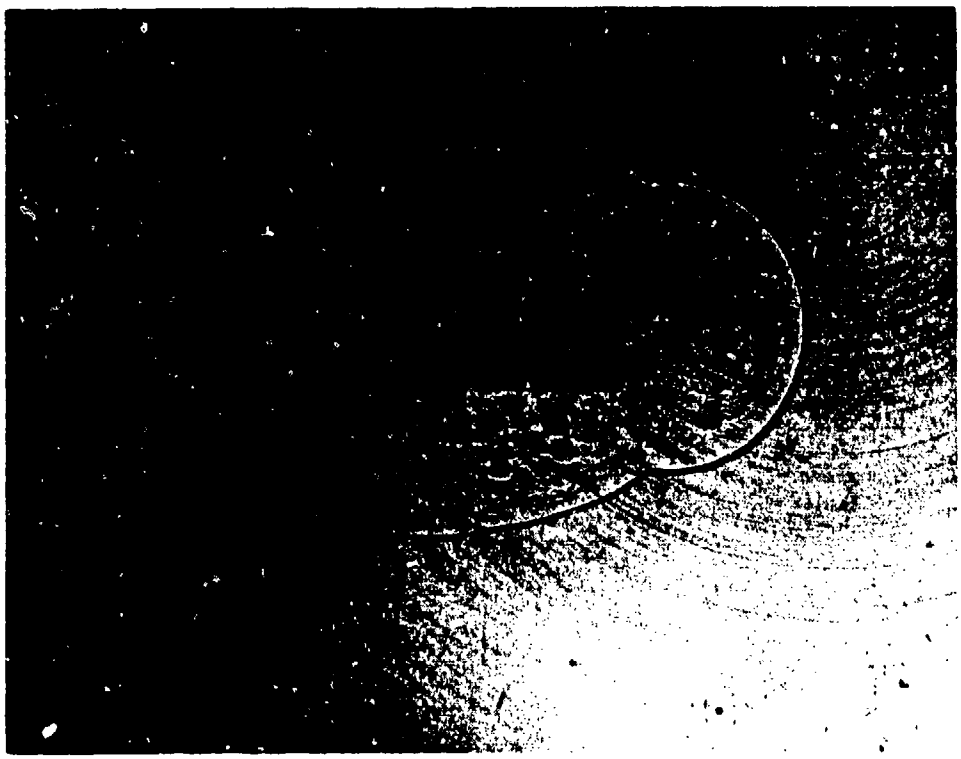

Figure 6. Spark Shadowgraph of Flow Field -110 μs Device #1.

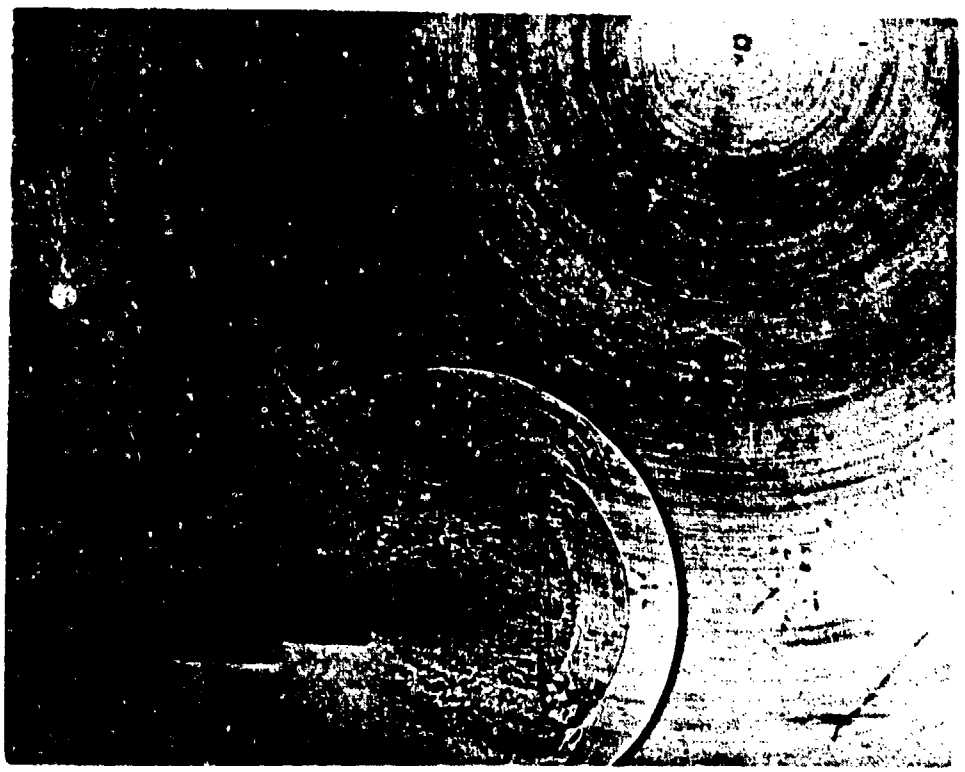

Figure 7. Spark Shadowgraph of Flow Field -14 μs Bare Muzzle.

Figure 8. Spark Shadowgraph of Flow Field -14 μs Device #1.

Figure 9. Spark Shadowgraph of Flow Field 139 μs Bare Muzzle.

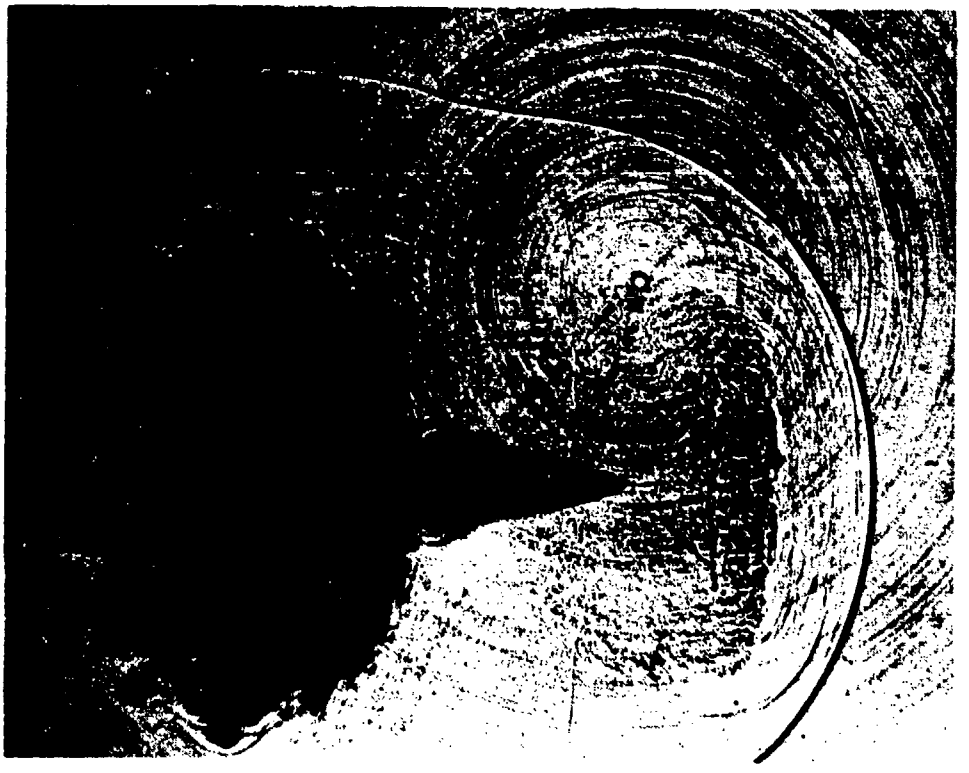

Figure 10. Spark Shadowgraph of Flow Field 139 μs Device #1.

Figure 11. Spark Shadowgraph of Flow Field 250 μs Bare Muzzle.

Figure 12. Spark Shadowgraph of Flow Field 250 μs Device #1.

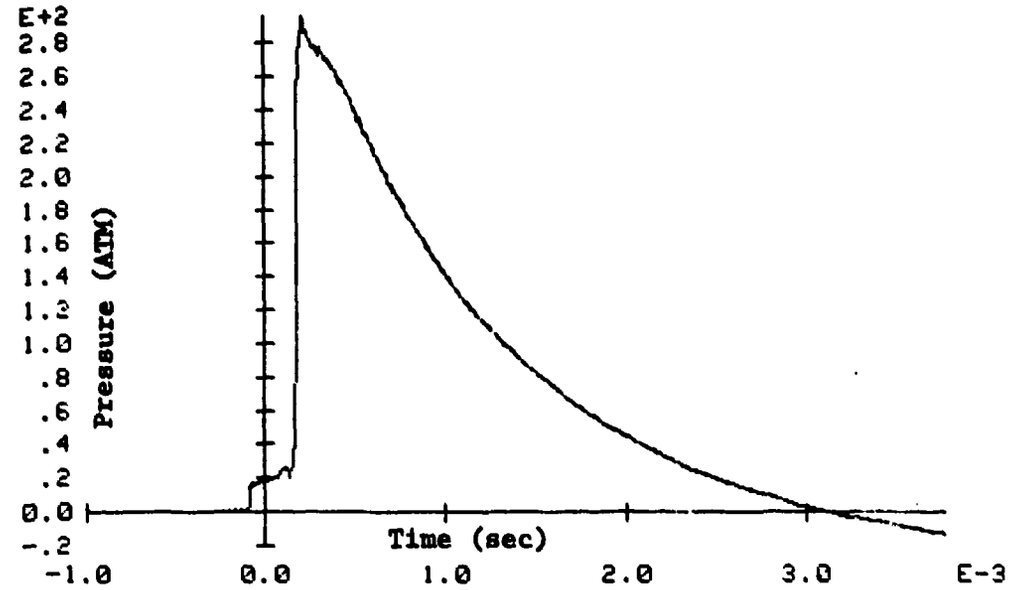

Figure 13. Static Internal Pressure Device #2, -.119 m from Muzzle.

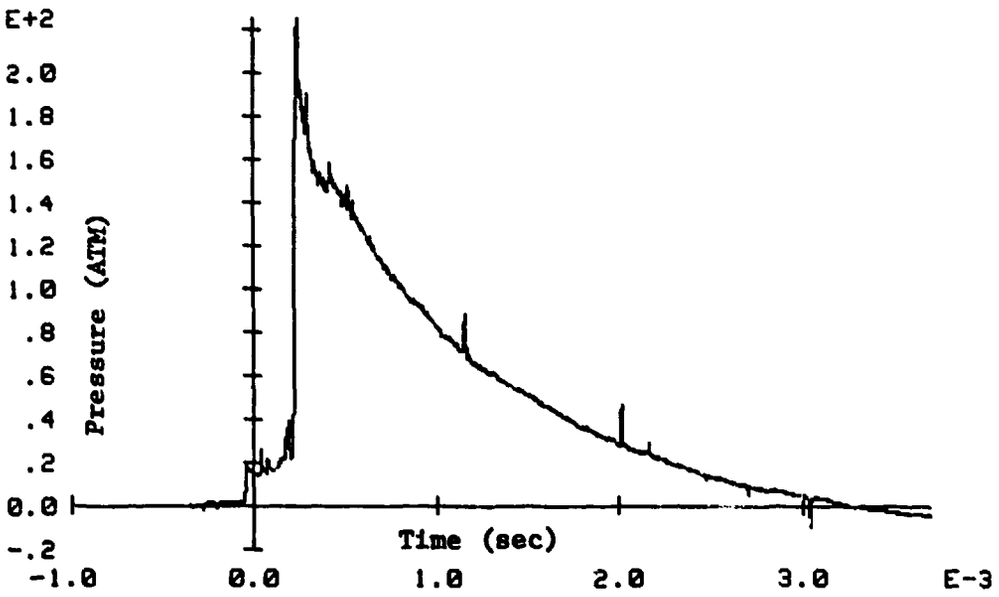

Figure 14. Static Internal Pressure Device #2, -.064 m from Muzzle.

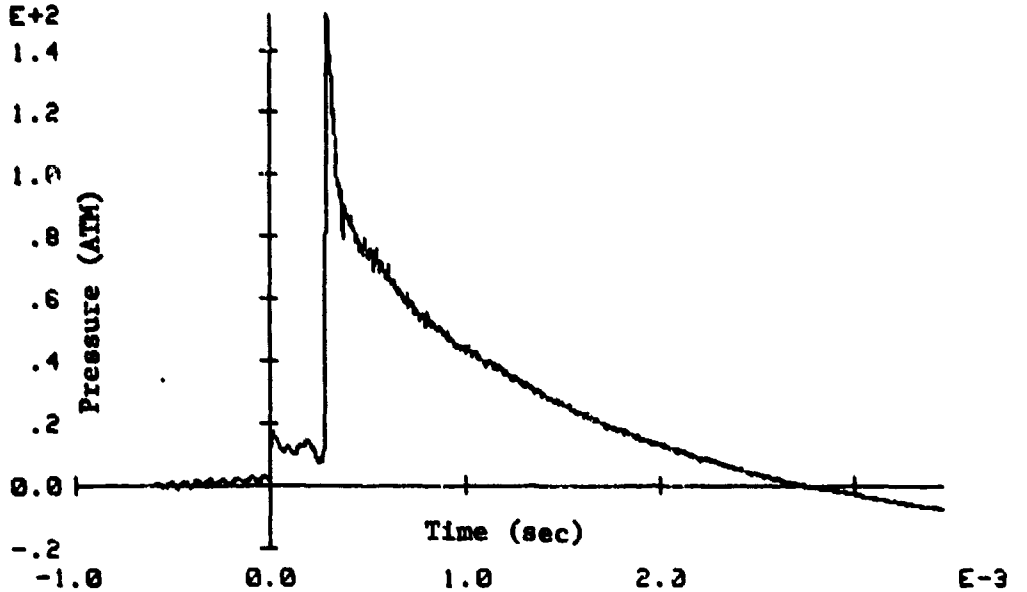

Figure 15. Static Internal Pressure Device #2, -.01 m from Muzzle.

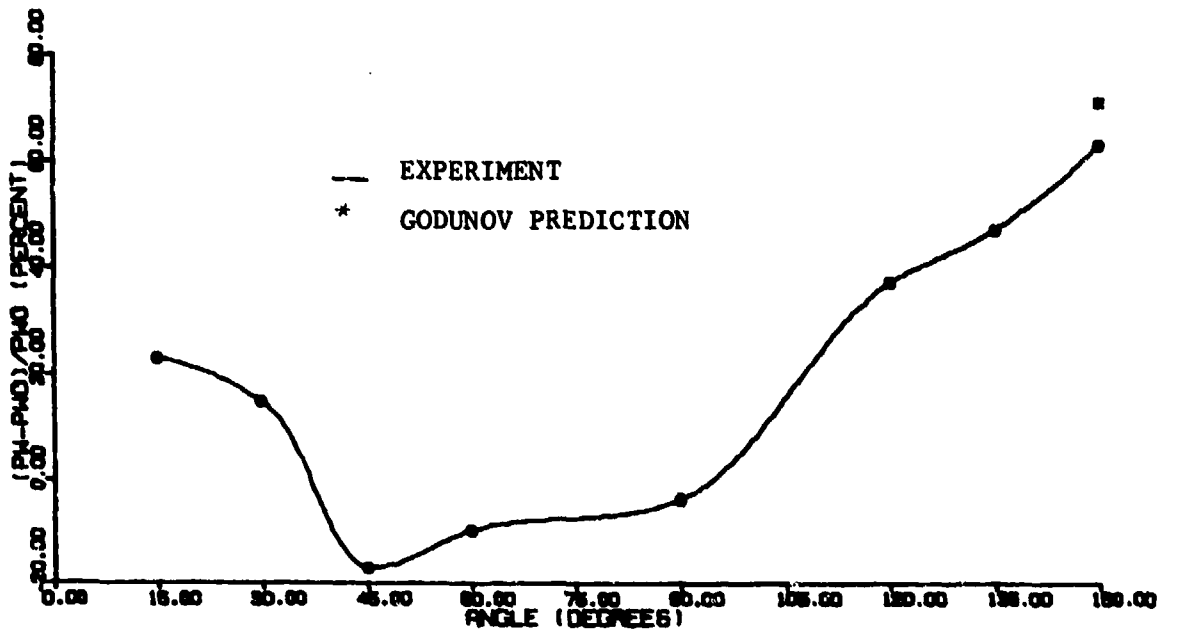

Figure 16. Comparison of Predicted and Measured Blast Overpressure Levels.

TECHNICAL REPORT INTERNAL DISTRIBUTION LIST

	NO. OF COPIES
CHIEF, DEVELOPMENT ENGINEERING BRANCH	
ATTN: DRSMC-LCB-D	1
-DP	1
-DR	1
-DS (SYSTEMS)	1
-DS (ICAS GROUP)	1
-DC	1
CHIEF, ENGINEERING SUPPORT BRANCH	
ATTN: DRSMC-LCB-S	1
-SE	1
CHIEF, RESEARCH BRANCH	
ATTN: DRSMC-LCB-R	2
-R (ELLEN FOGARTY)	1
-RA	1
-RM	1
-RP	1
-RT	1
TECHNICAL LIBRARY	5
ATTN: DRSMC-LCB-TL	
TECHNICAL PUBLICATIONS & EDITING UNIT	2
ATTN: DRSMC-LCB-TL	
DIRECTOR, OPERATIONS DIRECTORATE	1
DIRECTOR, PROCUREMENT DIRECTORATE	1
DIRECTOR, PRODUCT ASSURANCE DIRECTORATE	1

NOTE: PLEASE NOTIFY DIRECTOR, BENET WEAPONS LABORATORY, ATTN: DRSMC-LCB-TL, OF ANY ADDRESS CHANGES.

TECHNICAL REPORT EXTERNAL DISTRIBUTION LIST

	NO. OF COPIES
ASST SEC OF THE ARMY RESEARCH & DEVELOPMENT ATTN: DEP FOR SCI & TECH THE PENTAGON WASHINGTON, D.C. 20315	1
COMMANDER DEFENSE TECHNICAL INFO CENTER ATTN: DTIC-DDA CAMERON STATION ALEXANDRIA, VA 22314	12
COMMANDER US ARMY MAT DEV & READ COMD ATTN: DRCDE-SG 5001 EISENHOWER AVE ALEXANDRIA, VA 22333	1
COMMANDER ARMAMENT RES & DEV CTR US ARMY AMCCOM	
ATTN: DRSMC-LC(D)	1
DRSMC-LCE(D)	1
DRSMC-LCM(D) (BLDG 321)	1
DRSMC-LCS(D)	1
DRSMC-LCU(D)	1
DRSMC-LCW(D)	1
DRSMC-SCM-O (PLASTICS TECH EVAL CTR, BLDG. 351N)	1
DRSMC-TSS(D) (STINFO) DOVER, NJ 07801	2
DIRECTOR BALLISTICS RESEARCH LABORATORY ARMAMENT RESEARCH & DEV CTR US ARMY AMCCOM ATTN: DRSMC-TSB-S (STINFO) ABERDEEN PROVING GROUND, MD 21005	1
MATERIEL SYSTEMS ANALYSIS ACTV ATTN: DRSXY-MP ABERDEEN PROVING GROUND, MD 21005	1
COMMANDER US ARMY AMCCOM ATTN: DRSMC-LEP-L(R) ROCK ISLAND, IL 61299	1
COMMANDER ROCK ISLAND ARSENAL ATTN: SMCRI-ENM (MAT SCI DIV) ROCK ISLAND, IL 61299	1
DIRECTOR US ARMY INDUSTRIAL BASE ENG ACTV ATTN: DRXIB-M ROCK ISLAND, IL 61299	1
COMMANDER US ARMY TANK-AUTMV R&D COMD ATTN: TECH LIB - DRSTA-TSL WARREN, MI 48090	1
COMMANDER US ARMY TANK-AUTMV COMD ATTN: DRSTA-RC WARREN, MI 48090	1
COMMANDER US MILITARY ACADEMY ATTN: CHMN, MECH ENGR DEPT WEST POINT, NY 10996	1
US ARMY MISSILE COMD REDSTONE SCIENTIFIC INFO CTR ATTN: DOCUMENTS SECT, BLDG. 4484 REDSTONE ARSENAL, AL 35898	2
COMMANDER US ARMY FGN SCIENCE & TECH CTR ATTN: DRXST-SD 220 7TH STREET, N.E. CHARLOTTESVILLE, VA 22901	1

NOTE: PLEASE NOTIFY COMMANDER, ARMAMENT RESEARCH AND DEVELOPMENT CENTER, US ARMY AMCCOM, ATTN: BENET WEAPONS LABORATORY, DRSMC-LCB-TL, WATERVLIET, NY 12189, OF ANY ADDRESS CHANGES.

TECHNICAL REPORT EXTERNAL DISTRIBUTION LIST (CONT'D)

	NO. OF COPIES
COMMANDER US ARMY MATERIALS & MECHANICS RESEARCH CENTER ATTN: TECH LIB - DRXMR-PL WATERTOWN, MA 01272	2
COMMANDER US ARMY RESEARCH OFFICE ATTN: CHIEF, IPO P.O. BOX 12211 RESEARCH TRIANGLE PARK, NC 27709	1
COMMANDER US ARMY HARRY DIAMOND LAB ATTN: TECH LIB 2800 POWDER MILL ROAD ADELPHIA, MD 20783	1
COMMANDER NAVAL SURFACE WEAPONS CTR ATTN: TECHNICAL LIBRARY CODE X212 DAHLGREN, VA 22448	1

	NO. OF COPIES
DIRECTOR US NAVAL RESEARCH LAB ATTN: DIR, MECH DIV	1
CODE 26-27, (DOC LIB) WASHINGTON, D.C. 20375	1
COMMANDER AIR FORCE ARMAMENT LABORATORY ATTN: AFATL/DLJ	1
AFATL/DLJG EGLIN AFB, FL 32542	1
METALS & CERAMICS INFO CTR BATTELLE COLUMBUS LAB 505 KING AVENUE COLUMBUS, OH 43201	1

NOTE: PLEASE NOTIFY COMMANDER, ARMAMENT RESEARCH AND DEVELOPMENT CENTER, US ARMY AMCCOM, ATTN: BENET WEAPONS LABORATORY, DRSMC-LCB-TL, WATERVLIET, NY 12189, OF ANY ADDRESS CHANGES.